Proceedings of the 19th World Congress
The International Federation of Automatic Control
Cape Town, South Africa. August 24-29, 2014

IFAC

Interdependent Multi-objective Sizing and Control Optimisation of a Renewable Energy Hydrogen System

Gerhardus Human [*] George van Shcoor [**]
Kenneth R. Uren [***]

*DST HySA Infrastructure Centre of Competence, Faculty of
Engineering, North-West University, Potchefstroom, South Africa
(Tel: +2718 299 1978, e-mail: 20828179@nwu.ac.za)
** Unit for Energy Systems, Faculty of Engineering, North-West
University, Potchefstroom, South Africa (e-mail:
george.vanschoor@nwu.ac.za)
*** School of Electrical, Electronic and Computer Engineering, Faculty
of Engineering, North-West University, Potchefstroom, South Africa
(e-mail: kenny.uren@nwu.ac.za)

Abstract: This paper presents a sizing and control optimisation architecture for the design and evaluation of a small-scale stand-alone hybrid PV-wind-battery system for the production of hydrogen (H_2) using proton exchange membrane (PEM) technology. Three objectives are considered simultaneously namely cost, efficiency and reliability. For this task an optimisation approach is developed combining a single objective genetic algorithm (GA) with a multi-objective GA (MOGA) to optimise nine system sizing variables and six power management system control set-point variables. The nine sizing and six control variables are combined to form a solution vector. The optimisation algorithm searches the search space, with user defined boundaries, for non-dominated solution vectors. The result is a set of solution vectors which are useful in the selection of components for the design and evaluation of these systems. The optimisation approach developed sufficiently searches the bounded search space and provides results in the form of a set of non-dominated solution vectors. These results are useful in understanding how the different components of such a non-linear complex system affect each other as well as the three objectives considered in this study.

Keywords: renewable energy, hydrogen production, multi-objective optimisation, sizing, control

1. INTRODUCTION

Hybrid renewable energy (RE) H_2 systems have non-linear complex characteristics and a large number of design variables. The sizing of these systems is dependent on time of day, local weather conditions, operating policy, and economic data (Human et al. (2012)). Throughout literature these systems are usually minimised for cost as is seen in a review by Fadaee and Radzi (2012). Optimising for cost negatively affects the expensive components such as the PEM electrolyser employing platinum catalysts. A limited number of studies evaluate additional objectives such as CO_2 emissions, and/or unmet load [UL]. Bernal-Agustín and Dufo-López (2009a) performed interdependent control and multi-objective sizing optimisation with objectives being cost, CO_2 emissions, and UL. Control optimisation included cost only with a different cost objective function. Early on Seeling-Hochmuth (1997) recognised the need to consider other objectives such as efficiency and reliability. It is evident from both works mentioned above that the sizing and control variables are interdependent and influence one another as well as all three of the objectives. Classical optimisation techniques have been introduced in the field

of renewable energy systems. These are computationally expensive and do not allow for the consideration of large, complex systems with many system variables. Heuristic optimisation algorithms in the field of RE systems have become increasingly common and are applied in numerous research works as is seen in Banõs et al. (2011). The most popular heuristic optimisation algorithms are listed in Fadaee and Radzi (2012) to be the GA and particle swarm optimisation (PSO). The GA is selected for this study for it's flexibility, ease of implementation on non-differentiable functions, working with discrete search spaces, and solving of global optimisation problems.

Wind and solar energy resources are considered by Moriarty and Honnery (2007) to be the only viable solution for H_2 production while Carmo et al. (2013) shows that proton exchange membrane (PEM) based electrolysis is the preferred technology for H_2 production from intermittent RE sources. PEM technology poses some drawbacks when operated with intermittent RE as seen in Sherif et al. (2005). In order to mitigate these drawbacks Li et al. (2009) shows that the combination of a high cost, high efficiency, short term LAB storage, with less efficient long term H_2 storage systems, capable of storing large

amounts of energy inexpensively, is the optimal solution. Both the PEM electrolyser, and LAB have efficiency and reliability considerations when subjected to intermittent operation. Additionally both the control and sizing of components have an effect on system cost, efficiency, and reliability, making sizing and control optimisation interdependent. Although these systems are expensive and have comparatively low efficiencies, Nelson et al. (2006) states that on-going research and improving system efficiency will make this technology economically viable in future. Various optimisation software packages are available for RE system simulation. These are given in Bernal-Agustín and Dufo-López (2009b) with very little of these packages including H_2 components and even less having optimisation capability.

In this paper an optimisation approach integrating both single and multi-objective optimisation techniques is developed and implemented. A single objective GA optimising six control variables is implemented in cascade with a MOGA, optimising nine sizing variables. The purpose of the optimisation approach is to find a set of non-dominated solution vectors which is useful for the design and evaluation of systems with similar configurations. The paper is outlined as follows: A description of the RE system is provided next in section 2. This is followed by a detail description of the developed optimisation approach including a brief description of the system model in section 3. Detail of the optimisation objectives is also given. Section 4 presents results obtained from the initial optimisation exercise. Results presented here only demonstrate the functionality of the optimisation approach developed. Detail analysis of the findings is to be presented following further progress.

2. SYSTEM DESCRIPTION

The system consist of a wind turbine (WT) generator, photovoltaic (PV) generators, a PEM electrolyser, and LAB storage. Back-up diesel generator or grid-tie connection is not considered and thus 100 % of the energy is to be supplied by the RE sources. This combination of components is the most common from a review of literature and existing systems from Fadaee and Radzi (2012). The configuration of the system considered in this paper is illustrated in Fig. 1. The WT and PV sources generate power and converted through a power conversion device to a DC bus. A DC bus is elected as both the batteries and PEM electrolyser operate with DC voltage. The LAB bank is managed by a charge controller which supplies energy when the RE sources are not sufficient, and stores energy when there is a surplus of RE. The power between the various devices is managed through a power management system for which the control set-points are optimised. Sizing variables optimised include PV slope, PV module series and parallel connections; WT power rating; PEM electrolyser operating voltage, current density, and membrane area; and LAB Ah rating and series and parallel connections. Control variables optimised include minimum and maximum battery SOC; electrolyser minimum and maximum current densities; and two scaling variables to control the power flow between the LABs and electrolyser. In this paper only the production of H_2 from RE and
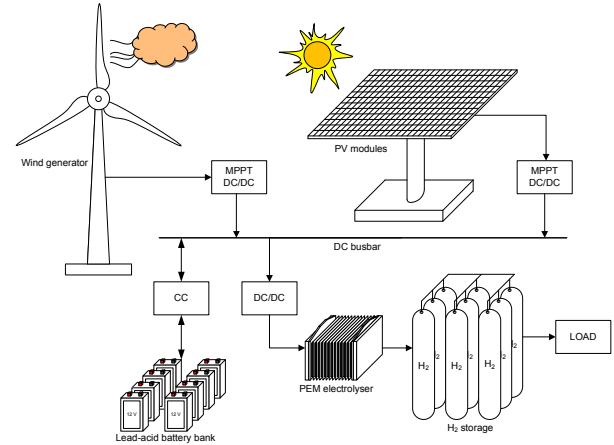

Fig. 1. Schematic of the PV-WT-LAB H_2 production system

not the usage is considered. H_2 production and usage are considered to be decoupled through its storage.

3. OPTIMISATION

3.1 Multi-objective optimisation

The standard form for a multi-objective problem is given by minimising objective function vector

$$
\begin{aligned}
&& \mathrm{F}(\bar{x}) = \{\mathrm{f}_1(\bar{x}), \dots, \mathrm{f}_K(\bar{x})\}, && \\
&\text{where} & \bar{x} = \{x_1, \dots, x_n\}, && \\
&\text{for} & g_j(\bar{x}) \leq 0, & j = 1, \dots, m & (1) \\
&& h_k(\bar{x}) = 0, & k = 1, \dots, p & \\
&& x_{iL} \leq x_i \leq x_{iU}, & i = 1, \dots, n,
\end{aligned}
$$

where $F(\bar{x})$ is the set of K objective functions, $\bar{x}$ represents the n-dimensional decision variable vector, and $g_j(\bar{x})$ and $h_k(\bar{x})$ respectively are m-dimensional inequality and p-dimensional equality constraint functions. Decision variables are restricted by upper and lower bound values, $\bar{x}_{iU}$ and $\bar{x}_{iL}$. The objective is to find a vector $\bar{x}^*$ in the solution space $\bar{X}$ that optimises the K objective functions.

Pareto optimality is essential in solving multiple objective problems. A Pareto optimum set is defined as a set of solutions which are non-dominated, meaning that for a set of Pareto solution vectors, there exists no other solution vector in the entire solution set that results in the improvement of at least one objective fitness value without a deterioration of the remaining objective fitness values. Fig. 2 illustrates a set of possible solutions for an optimisation problem considering the two minimising objectives f_1 and f_2. Solutions "1" to "5" are non-dominated solution vectors lying on the Pareto front. These solution vectors form the Pareto optimal set. Solution vectors 6 to 15 are dominated and do not form part of the Pareto optimal set.

3.2 System model

System design, analysis, and optimisation requires a mathematical system model. The model is developed in the Matlab$^{\circledR}$ and Simulink^{TM} simulation environments and constructed from individual component models integrated into a single system simulation. Components modelled
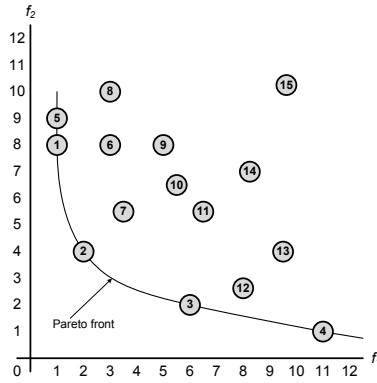
Fig. 2. Illustration of the Pareto optimal front.

include PV cells, WT generator, LAB, PEM electrolyser, power electronic converters, and power management system. For the optimisation exercise the models are required to be generic. Models selected include the main component dynamics which affects component efficiency and reliability. The PEM electrolyser and LAB are identified to have reliabilities affected by the sizing and control parameters and for that reason these two components are modeled to include reliability components.

Wind speed and irradiation data use statistical distributions to simulate the inputs. Irradiation input data available for the site is monthly average daily irradiation measured on a horizontal surface. Using distributions from Bendt et al. (1981) an average monthly clearness index is determined and finally hourly irradiation on a tilted surface (G[kW/m^2]). Clearness index (k_T) is the relationship between the terrestrial and extraterrestrial radiation. Extraterrestrial radiation is calculated from the work of Duffie and Beckman (1991). Wind distributions use a Weibull distribution function described in Borowy and Salameh (1994). Shape and scale factors for the Weibull distributions are derived from available measured data and in turn used to generate a wind speed distribution profile.

PV cell characteristics have a strong dependency on solar radiation and module temperature. The PV model implemented is a single diode equivalent circuit model providing voltage-current characteristics and is referred to as the four parameter model described in Duffie and Beckman (1991). A lumped thermal model given in Lebbal and Lecoeuche (2009) is included. Power from a WT is mainly dependent on wind speed and hub height. The instantaneous value of power in the wind, P_w, is given by

$$P_w = \frac{1}{2}\rho V^3 C_p, \tag{2}$$

with V the wind speed [m/s] and C_p the fraction of upstream wind power captured by the rotor blades. Most models from literature are empirical models using rated power, cut-in-, cut-out-, and rated-wind speeds to provide the power from a WT as a function of the wind speed. For this work the power-wind speed curve from a commercially available 3kW turbine is normalised. This ensures that the WT model remains generic by multiplying the normalised power-wind speed curve values with the component rating.

The LAB performance model implemented is the CIEMAT model discussed in detail by Gergaud et al. (2003). Addi-

tionally a cycle-counting algorithm implemented by Bindner et al. (2005) is added to incorporate a reasonable accurate lifetime model for reliability calculations. The generic property of the CIEMAT model makes it appropriate for optimisation exercises. Battery voltage-current relationship is modelled as a function of battery rating, state of charge (SOC), charge and discharge currents, and temperature. This model includes gassing voltage and end of charge voltage. Battery life is modelled by an adoption of Miner's rule which involves a combination of conventional battery lifetime information from the data sheet and a cycle counting algorithm that determines the number of cycles from the depth of discharge (DOD). Number of cycles vs. DOD data is provided by battery manufacturers and imported into a lookup table. The fractional life used in a given cycle is calculated to be $1/C_F$ where C_F is the fractional discharge. End of battery life is defined as the point where the battery has reached 80 % of the nominal capacity. When the sum of the fractional life values add up to 20 % the battery life is considered to be over and requires replacement.

The PEM electrolyser model is an electrochemical model described in detail in Carmo et al. (2013). The model provides the voltage-current relationship for specific electrolyser parameters as voltage drops across the electrolyser components. The model includes temperature effects with a lumped parameter temperature model from Lebbal and Lecoeuche (2009). For the power conversion device a generic three parameter model from Ulleberg and Glockner (2002) is implemented which relates the input power to the output power as a function of output voltage. The model is based on empirical efficiency curves and is numerically robust and generic. The model requires three parameters obtained from power curves. The three parameters used are obtained from work done in Ulleberg and Glockner (2002).

The power controller distributes power between the different components based on predefined criteria for several operating modes denoted OM0 (off mode), OM1, OM2, OM3, OM4, OM12, OM13, and OM14. Each operating mode is subject to the state of six conditions shown in Fig. 3, numbered one to six in the diamond shaped decision blocks. Actions as a result of these conditions are based on controller set-points which are the optimised control variables.
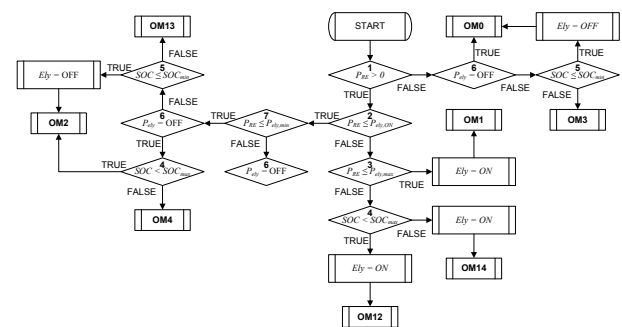

Fig. 3. Power controller logic diagram

3.3 Optimisation architecture

The sizing and control optimisation architecture implemented in the current work comprises of a single-objective algorithm and a multi-objective algorithm both optimising for the same objective functions: efficiency, cost, and reliability. Control optimisation implements a single objective GA while sizing optimisation implements a MOGA. For both sizing and control all three objectives are evaluated. The first objective is evaluated for control while all three objectives are evaluated for sizing. When the optimisation criteria are met, the second objective is evaluated for control with all three objectives evaluated for sizing again. This is repeated for the third objective. The result is three Pareto optimal sets, each having control variables optimised for one objective at a time. These are combined to form a single set of non-dominated Pareto optimal solutions. The flow of the optimisation approach developed is given in Fig. 4. A description of each of the steps is
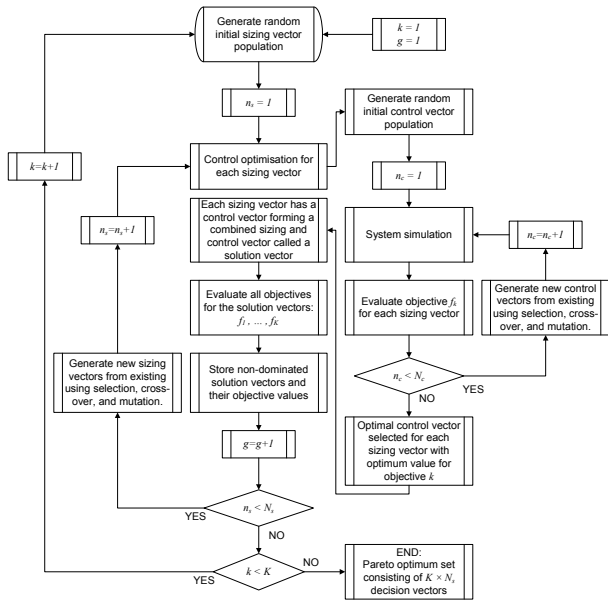

Fig. 4. Optimisation flow diagram.

provided next:

(1) Set objective function to first objective, $k = 1$, and start the first iteration, $g = 1$.
(2) Generate initial random set of sizing vectors.
(3) Optimise control for objective function $f(k)$ using the single objective GA for each sizing vector.
  (a) Generate random initial set of control vectors.
  (b) Calculate fitness values for each vector for objective function $f(k)$.
  (c) Implement operators: selection, crossover, and mutation.
  (d) Repeat GA until number of generations or set-point tolerance is achieved.
(4) Calculate fitness values for all objectives functions $(f_1, \ldots, f_K)$.
(5) Determine non-dominance of the current solution vectors.
(6) Store non-dominated objective function values and corresponding solution vectors.

(7) Implement operators: selection, crossover, and mutation.
(8) Repeat steps (3) to (7) for N_s generations.
(9) Select the next objective function for control optimisation, $k = k + 1$.
(10) Repeat steps (2) to (9) K times to optimise all objective functions for control.
(11) At the end of the optimisation exercise the Pareto solution set contains a maximum of $g = N_s \times K$ solution vectors for evaluation of both sizing and control.

3.4 Objective functions

The objectives to be minimised are the negative of the average system efficiency per annum [%], the total life-cycle cost (TLCC) per kilogram of produced H$_2$ [R/kg], and the inverse of the overall system reliability based on reliability indicators of the electrolyser and LAB bank. Determining these objectives is the topic of the paragraphs to follow.

Efficiency is determined to be the average system efficiency measured over a simulation period of one year. It is defined as the ratio of energy available in the H$_2$ produced by the system to the input energy from the renewable energy sources and is given by

$$\eta_{system} = \frac{E_{out}}{E_{in}}. \tag{3}$$

The objective function to be minimised is the negative of efficiency given by

$$f_1 = -\eta_{system}. \tag{4}$$

Cost is determined as the TLCC of the system per kilogram of H$_2$ produced for a 25 year lifetime. TLCC discounts all costs through the lifetime of the system to an equivalent present value which includes initial, operation and maintenance (O&M), and replacement costs. The financial model used is from Farr (2011). Component economic specifications along with component expected lifetimes are provided in Table 1.

Table 1. Component economic specifications.

Component	PV	WT	Ely	LAB	PCD
C_i [R/W]	3.6	21.7	10	2.15	6.5
$C_{O\&M}$ [%]	1	1	2	1	1
Life [yr]	25	25	10	4	10

Total cost per component is calculated by

$$C_{comp} = C_I + C_{O\&M} + C_R \tag{5}$$

with C_I the sum of the component initial investment, $C_{O\&M}$ O&M cost, and C_R the replacement costs. Initial investment cost per component is calculated for the PV by

$$C_I = C_i \times N_{comp}, \tag{6}$$

with C_i the normalised PV cost [R/module] and N_{comp} the number of PV modules. For all other components the initial investment cost is calculated using

$$C_I = C_i \times P_{comp}, \tag{7}$$

with C_i the normalised component cost [R/W] and P_{comp} the rating of the component [W]. O&M cost per component is calculated by

$$C_{O\&M} = C_{O\&M_0} \times C_I \times \frac{(1+d)^Y - 1}{d(1+d)^Y}, \tag{8}$$

with $C_{O\&M_0}$ the O&M cost in the first year, d the discount rate, and Y the lifetime in years of the system. Replacement costs are calculated by

$$C_R = C_I \times (1+d)^{-Y}. \tag{9}$$

The final system cost per kilogram $[m_{H_2}]$ is the sum of the cost of all components over the lifetime of the system divided by the amount of H_2 produced for the same period. The objective function to be minimised is the sum of all the component costs given by

$$f_2 = \frac{\sum C_{comp}}{m_{H_2}}. \tag{10}$$

Reliability is the probability that a system or component will accomplish its designated task over a period of time when subjected to specified operating conditions. The current work is not concerned with the probability of a component failure, but rather requires a relative indication of the contribution to degradation as a result of operating actions known to contribute to degradation. Reliability in this case is redefined as the quantification of certain identified degradation mechanisms for a component subjected to intermittent operation. The PEM electrolyser and LAB are the components that degrade due to operating conditions. The life expectancy of a LAB is measured in number of cycles which is dependent on the depth-of-discharge. A cycle counting algorithm calculates the percentage LAB capacity lost per annum with LAB reliability given by

$$R_{BB} = exp\left(-q_{LAB_{lost}}\right), \tag{11}$$

with $q_{LAB_{lost}}$ the average capacity lost between the two banks. Electrolysers have a terminal voltage increase as a result of degradation inside the electrolyser. Clarke et al. (2009) attributes rapid electrolyser degradation to the highly fluctuating power input. The extent to which lifetime degradation is directly contributed to variability in power input, is to date not quantified. Ulleberg (1998) uses number of starts and average run time to compare simulation for different operating strategies. Electrolyser reliability is therefore related to the average on-time given by

$$R_{ely} = exp(-T_{ely,max} + T_{ely,avg}), \tag{12}$$

with $T_{ely,max}$ the maximum possible on-time per cycle for each specific site and $T_{ely,avg}$ the actual measured average on-time per cycle. Both components are essential for the system to function properly and is considered a series network with the overall system reliability given by the multiplication of battery and electrolyser reliabilities. The objective function to be minimised is the inverse of the overall system reliability given by

$$f_3 = (R_{ely} \times R_{BB})^{-1}. \tag{13}$$

4. RESULTS

Several runs of the optimisation approach are performed, each having a Pareto optimal set of solution vectors. In this paper all solution vectors are combined and the non-dominated solutions eliminated to form a single Pareto optimal set. This Pareto set is illustrated for all three objectives in Fig. 5. The density of solution vectors on
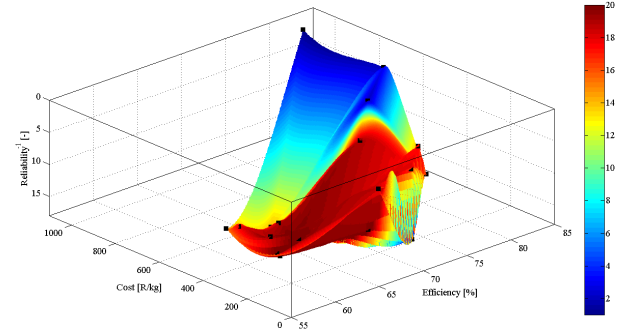

Fig. 5. Pareto front for the three objectives.

the Pareto front is determined to evaluate the ability of the optimisation approach to adequately search the entire search space. For each solution vector $(F_1,\ldots,F_b)$ on the Pareto front the average normalised distance to all other solution vectors is determined with the minimum of these averages selected as a closed ball defined by

$$\tilde{B}(F_{b_0}, r) = \{F_b \epsilon \mathbb{R} | d(F_b, F_{b_0}) \le r\}, \tag{14}$$

for b solution vectors, with F_{b_0} the centre of the closed ball, and d the distance function which associates a distance $d(F_b, F_{b_0}) = |F_b - F_{b_0}|$ for every pair of solution vectors. For each solution vector (F_{b_0}) the number of solution vectors with $d \le r$ is counted providing a measure of solution vector density on the Pareto front.

The colour of the graph indicates the spread of solution vectors over the Pareto front and is directly related to the number of solution vectors inside each closed ball defined by (14) and indicated by the colour bar in Fig. 5. Dark red areas are densely populated while blue areas are sparsely populated. This is a result of the optimisation approach converging to non-dominated solutions. Solutions with at least one optimum objective value has a higher probability of being dominated and this is visible in the graph. For a better illustration of the results and analysis of the Pareto set, the objective function values for f_3 for for the Pareto set are grouped from low to high into five equal groups and plotted against f_1 and f_2 in Fig. 6. Low values for f_3 (lower 20 % of values) corresponds to low cost and low efficiency while the high values for f_3 (upper 81 - 100 % of values) correspond to high efficiency and also high cost. For these results the optimal zone would be 50 - 60 % efficiency, resulting in relatively moderate cost and low inverse reliability.

5. CONCLUSIONS AND FUTURE WORK

This paper presents an optimisation approach for the combined control and sizing optimisation of a small-scale stand-alone hybrid PV-wind-battery system for the production of H_2 using PEM technology. Control and sizing
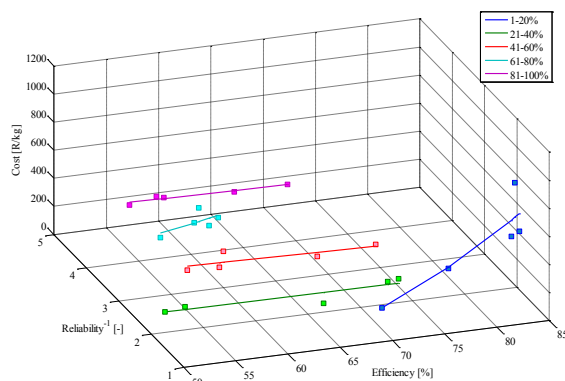
Fig. 6. Cost vs. efficiency for five ranges of inverse reliability with trend lines.

parameters are evaluated for the three objectives, cost, efficiency, and reliability. A system model including power control is developed in the Matlab® and Simulink^{TM} simulation environment. A smalls-scale stand-alone RE system is evaluated. From the distribution of solution vectors on the Pareto front it is shown that the optimisation approach converges to an isolated area on the Pareto front indicating that there is an optimal zone from which solutions can be determined based on the relative importance of the objectives. From the results the expected conflicting nature of the objectives selected, especially the cost and efficiency, is clearly visible. Ongoing research includes refining the optimisation process, both in execution time and locating minima on the Pareto front. Future work will include a Pareto front sensitivity analysis to determine the control and sizing parameters it is most sensitive for. The results are to be evaluated using multivariate statistical analysis techniques. Furthermore a comparison with other commonly used optimisation algorithms such as particle swarm optimisation is also warranted.

ACKNOWLEDGEMENTS

REFERENCES

Banõs, R., Manzano-Agugliaro, F., Montoya, F., Gil, C., Alcayde, A., and Gmez, J. (2011). Optimization methods applied to renewable and sustainable energy: A review. *Renewable and Sustainable Energy Reviews*, 15(4), 1753 – 1766.

Bendt, P., Collares-Pereira, M., and Rabl, A. (1981). The frequency distribution of daily insolation values. *Solar Energy*, 27(1), 1 – 5.

Bernal-Agustín, J.L. and Dufo-López, R. (2009a). Multi-objective design and control of hybrid systems minimizing costs and unmet load. *Electric Power Systems Research*, 79(1), 170 – 180.

Bernal-Agustín, J.L. and Dufo-López, R. (2009b). Simulation and optimization of stand-alone hybrid renewable energy systems. *Renewable and Sustainable Energy Reviews*, 13(8), 2111 – 2118.

Bindner, H., Cronin, T., Lundsager, P., Manwell, J.F., Abdulwahid, U., and Baring-Goould, I. (2005). Lifetime modelling of lead acid batteries. Technical Report Risø-R-1515, Risø National Laboratory, Roskilde, Denmark.

Borowy, B. and Salameh, Z. (1994). Optimum photovoltaic array size for a hybrid wind/pv system. *Energy Conversion, IEEE Transactions on*, 9(3), 482 –488.

Carmo, M., Fritz, D.L., Mergel, J., and Stolten, D. (2013). A comprehensive review on {PEM} water electrolysis. *International Journal of Hydrogen Energy*, 38(12), 4901 – 4934.

Clarke, R., Giddey, S., Ciacchi, F., Badwal, S., Paul, B., and Andrews, J. (2009). Direct coupling of an electrolyser to a solar pv system for generating hydrogen. *International Journal of Hydrogen Energy*, 34(6), 2531 – 2542.

Duffie, J. and Beckman, W. (1991). *Solar Engineering of Thermal Processes.* A Wiley-Interscience Publication. John Wiley & Sons.

Fadaee, M. and Radzi, M. (2012). Multi-objective optimization of a stand-alone hybrid renewable energy system by using evolutionary algorithms: A review. *Renewable and Sustainable Energy Reviews*, 16(5), 3364 – 3369.

Farr, J.V. (2011). *Systems Life Cycle Costing: Economic Analysis, Estimation, and Management.* CRC Press.

Gergaud, O., Robin, G., Multon, B., Ahmed, H.B.E.N., Branch, S.B., Cachan, E.N.S.D., Lann, K., and France, B. (2003). Energy modeling of a lead-acid battery within hybrid wind photovoltaic systems. *Proc EPE*, 1–10.

Human, G., van Schoor, G., Uren, K.R., Venter, W.C., Grobler, A.J., Haultzhausen, J., Oelofse, S.P.O., van der Merwe, F., and Bessarabov, D. (2012). Design of a stadn-alone renewable energy hydrogen production system for distributed, small-scale applications in south africa. In *International Conference on Hydrogen Production.*

Lebbal, M. and Lecoeuche, S. (2009). Identification and monitoring of a pem electrolyser based on dynamical modelling. *International Journal of Hydrogen Energy*, 34(14), 5992 – 5999.

Li, C.H., Zhu, X.J., Cao, G.Y., Sui, S., and Hu, M.R. (2009). Dynamic modeling and sizing optimization of stand-alone photovoltaic power systems using hybrid energy storage technology. *Renewable Energy*, 34, 815 – 826.

Moriarty, P. and Honnery, D. (2007). Intermittent renewable energy: The only future source of hydrogen? *International Journal of Hydrogen Energy*, 32, 1616 – 1624.

Nelson, D., Nehrir, M., and Wang, C. (2006). Unit sizing and cost analysis of stand-alone hybrid wind/PV/FC power generation systems. *Renewable Energy*, 31, 1641 – 1656.

Seeling-Hochmuth, G.C. (1997). A combined optimisation concept for the design and operation strategy of hybrid-pv energy systems. *Solar Energy*, 61(2), 77 – 87.

Sherif, S., Barbir, F., and Veziroglu, T. (2005). Wind energy and the hydrogen economy–review of the technology. *Solar Energy*, 78(5), 647 – 660. Solar Hydrogen.

Ulleberg, O. (1998). *Stand-alone power systems for the future: Optimal design, operation & convtrol of solar-hydrogen energy systems.* Ph.D. thesis, Norweigian University of Science and Technology, Trondheim.

Ulleberg, O. and Glockner, R. (2002). Hydrogems - hydrogen energy models. In *14th World Hydrogen Energy Conference.*